RESEARCH ARTICLE-MECHANICAL ENGINEERING

The influence of abrasive size and applied load on abrasive wear of Al-Si–SiCp composite

Raj Kumar Singh[1] · Amit Telang[2] · Satyabrata Das[3]

Abstract

The abrasive wear response of Al-7.5Si–SiC composite produced by stir casting technique was examined and compared to Al-7.5Si alloy (matrix alloy) and Al-17.5Si (low-cost hypereutectic) alloy in as-cast and after heat treatment. The microstructure of the hypereutectic alloy shows the α-Al, α-Si, and Al-Si eutectic phases, and the microstructure of the composite shows the homogeneous dispersion of SiCp in the matrix and excellent bonding of the Al-SiC interface. The wear examinations were performed on pin-on-disc apparatus at 38–80 μm abrasive (grit) sizes, 5–20 N applied loads, 100–400 m sliding (abrading) distances, and 1 m/s constant sliding speed. At 80 μm size of abrasive and 20 N of the applied load, the decrement in wear rate of LM30 alloy and LM25-SiCp composite was 31.82% and 95.37%, respectively, in case of the as-cast condition. However, for heat-treated conditions, the decrement in wear rate of hypereutectic alloy and composite was 32.63% and 96.61%, respectively. The wear rate of specimens was increased with abrasive size and applied load. The wear resistance of the hypereutectic alloy was superior to the matrix alloy but inferior to the composite irrespective of the abrasive size and applied load. The wear surface of the specimens, abrasive papers, and wear debris were analysed by the field-emission scanning electron microscope (FESEM) for the wear mechanism.

1 Introduction

Aluminium alloys are enormously used in several engineering applications, including aerospace, automotive, marine, and military [1, 2] Because of their superior characteristics like excellent stiffness, low density, and exceptional corrosion resistance. However, the inadequate tribological response is the major drawback of aluminium alloys. The dispersion of hard ceramic particles in aluminium alloys, known as aluminium matrix composite (AMCs), overcome this problem. AMCshave an outstanding combination of proper-

ties such as superior wear resistance, greater specific strength, greater specific stiffness, higher damping capacity, improved high-temperature strength, and controlled coefficient of thermal expansion compared to unreinforced aluminium alloys [3, 4]. By variation of the content of reinforcements in the matrix materials, the properties of aluminium matrix composites can be tailored to meet the specific applications. It is described that Al-10%SiCp composite gives comparable mechanical properties while improved specific heat and thermal conductivity compared to cast iron [5, 6]. Günay and Şeker [7] examined the machining behaviour of tungsten carbide (WC), cubic boron nitride (CBN), and polycrystalline diamond cutting tools relating to the surface roughness of Al-Si-SiC composite. They found that polycrystalline diamond is the best cutting tool compared to other cutting tools for surface improvement of the materials. The surface roughness of the materials is reduced with cutting speeds increased irrespective of the cutting tools materials. Wang et al. [8] found that the heat treatment and hot rolling process improved the hardness, ultimate tensile strength, and yield strength of the Al-11.73 Mg-6.63Si-0P and Al-11.73 Mg-6.63Si-0.05P composites. This was caused by the

✉ Raj Kumar Singh
raju_tit@yahoo.co.in

1 Department of Mechanical Engineering, Rewa Engineering College, University Road, Rewa, Madhya Pradesh 486002, India

2 Department of Mechanical Engineering, Maulana Azad National Institute of Technology, Link Road Number 3, Bhopal 462003, India

3 Department of Material Science and Metallurgical Engineering, Maulana Azad National Institute of Technology, Link Road Number 3, Bhopal 462003, India

refinement of Mg2Si particles, subgrains and sharped edge precipitates. The Al-11.73 Mg-6.63Si-0.05P composite has higher wear resistance and lower coefficient of friction than the Al-11.73 Mg-6.63Si-0P composite because of increased hardness and refined Mg_2Si phase. Alizadeh and Taheri-Nassaj [9] investigated the influence of B_4C nanoparticle contents on the mechanical properties and wear behaviour of Al–Cu alloy. The results exhibited that the composites had excellent wear resistance, yield strength, hardness and decreased ductility by adding 2 and 4 wt.% B_4C nanoparticles into the matrix. Vencl et al. [10] concluded that the cluster formation of Al_2O_3 and SiC particles was seen in the microstructure of the composites. The cluster of SiC particles in the composite was more favourable than the Al_2O_3 particles for mechanical and wear properties. The matrix alloy (hypoeutectic A356 alloy) was fractured in a ductile manner, whereas the composite was fractured a transition from ductile to brittle, and the intergranular fracture was observed in the reinforcing particles region. The wear resistance of the Al-Si-SiC composite was superior, and the friction coefficient was inferior to the Al-Si-Al_2O_3 composite because of the greater hardness of the SiCp. Abdizadeh et al. [11] investigated the effect of ZrO_2 particles and casting temperatures on the mechanical properties of A356-ZrO_2 composites. The results revealed that the hardness and ultimate tensile strength of the composite were superior to the matrix alloy. The fracture surface of the composite exhibited a similar fracture mechanism to the matrix alloy. The interdendritic cracking of the matrix is responsible for the failure of the materials. Many dimples were shown in the fracture surface of the materials; the crack nucleation and subsequent coalescence cause this during the fracture.

Consequently, the frictional temperature of these composite is considerably less than the cast iron [6]. For attaining durability, energy and materials saving, environmental and economic benefits, aluminium matrix composites are a suitable replacement for aluminium alloys, cast iron, and steels. Therefore, aluminium matrix composites are used in various engineering and automobile parts where seizure, wear, and tear are the main problems as well as the saving of weight. These parts are cylinder heads, brake drums, pistons, driveshafts, connecting rods for automobile fields and turbine blades, impellers, valves, vortex finder, and agitators for mining and marine fields. Nowadays, many components from aluminium matrix composites have reached the mercantile production stage [12–18]. Mostly, those parts are subjected to various types of wear and tear associated with deformation. Therefore, the characterisation of aluminium matrix composite is required concerning wear under different parameters.

Many researchers have investigated the adhesive wear response of aluminium matrix composites [7, 19–29], while a limited investigation has been done on abrasive wear response of AMCs [30–36]. Sahin [30–32] demonstrated

that the abrasive wear rate of the base material and composite increased with the abrading distance, abrasive size, and applied load for silicon carbide abrasive paper. The abrasive size and reinforcement size were the dominant parameters for wear of Al-Cu-SiCp composite; however, also found that the applied load and abrading distance will have no substantial influence on the wear properties of the materials. The coarser reinforcement size of the composite represented more excellent wear resistance than the finer reinforcement size of the composite. Mondal and Das [33] investigated the effect of applied load, size, and concentration of the dispersoid on the abrasive wear response of the Al-SiC composite. It was found that the composite has greater abrasive wear resistance than the base material. The wear rate of the specimens increases linearly with the applied load and invariant with the abrasive size of the abrasive paper. Sharma et al. [34] investigated the influence of solution-treated temperature during the T6 heat treatment process of as-cast Al-Si alloys with varying percentages of Si on two-body abrasive wear behaviour. It was observed that the Si contents and solution-treated temperature during T6 heat treatment significantly affected the wear properties. The wear resistance of the materials improved as the solution-treated temperature increased. The hypereutectic alloy (Al-16%Si) found excellent wear resistance than the eutectic alloy (Al-12%Si) and hypoeutectic alloy (Al-8%Si); also, similar results were found by Shah et al. [35]. Singh et al. [36] reported the influence of microstructure, mechanical properties, and abrading distance on the abrasive wear behaviour of LM30-10%SiC composite and its base alloy. It was found that the abrasive wear rate of specimens increases with an increase in the abrasive size and applied load but is invariant with the abrading distance.

The microstructure of the LM25–10%SiC composite mainly comprises of distribution of SiCp in the alloy matrix (Al-7.5%Si). It is well known that the microstructure of hypereutectic (LM30) alloy is comprised of a eutectic (Al-Si) matrix into which α-Si cuboids are distributed. The hypereutectic alloy (Al-17.5%Si) can support a similar microstructure in which SiCp are distributed in LM25 (Al-7.5%Si) alloy matrix. There are several opinions concerning the application of the low-cost hypereutectic alloy instead of the LM25–SiC composite. Additionally, α-Si is distributed in the Al-Si eutectic matrix, and it is felt that the mechanical properties and wear response of the composite would be like the hypereutectic alloy. To ascertain the validity of this concept, comprehensive research work is required to compare the properties of LM25–SiC composite and low-cost hypereutectic alloy [37]. Singh et al. [37] recently reported the influence of abrading (sliding) distance on wear response of Al-Si-SiCp composite compared to the base material and hypereutectic alloy in both as-cast and after heat-treatment. It is noted that the study is essential to ascertain the effect of different abrasive sizes and applied load on wear properties.

Against this background, the present study was the extension of previous research work [37] in understanding the influence of abrasive (grit) size of the abrasive paper and applied load on high-stress abrasive wear behaviour of LM25-SiC composite, comparing with as-cast and heat-treated base alloy and low-cost hypereutectic (LM30) alloy.

2 Experimental Section

2.1 Material Preparation

The Al-Si (LM25 and LM30) alloys and LM25 alloy containing 10 wt% SiC particles were selected in the current research work. The chemical compositions (in wt%) of the LM25 alloy and LM30 alloy are 7.5Si–0.5 Mg–0.5Fe–0.2Cu, and the balance is Al and 17.5Si–4.5Cu–0.6 Mg–1Fe–and balance is Al, respectively. The ingots of LM25 (matrix) alloy and LM30 (hypereutectic) alloy were melted in a graphite crucible at 750 °C using Coverall 11 (Make: Fosico India Ltd.) as a cover flux to avoid oxidation of aluminium alloy, stirring with the help of a mechanical stirrer and degassed by dry nitrogen gas and then skimmed off the dross floating on the liquid surface, and finally, the alloy melt was solidified into a permanent cast iron die. SiC particles were used for dispersing in the Al alloy because of its higher young's modulus (400 GPa), density is 3.1 g/cm^3 nearly equal to Al melt, compressive strength 3900 MPa, and maximum used temperature is around 1650 ^{O}C. The presence of SiC particles in the Al alloy melt enhanced the specific modulus, specific strength, thermal stability and improved the wear resistance. The SiC particles with the size of 20–40 μm were incorporated into the LM25 alloy melt by the stir-casting method (liquid metallurgical technique). In the stir casting technique, a specially designed stirrer was used made of stainless steel coated with graphite + sodium silicate paste. The stirrer was rotated at a speed of 650–700 RPM, which produced a vortex on the melt, and SiC particles were added to the vortex. As soon as the SiC particles were added to the vortex, the particles were sucked in the melt, and the stirring action mixed the particles in the melt. To induce the wettability between the melt and the SiC particles, Mg metal in 100 gm pieces was added to the melt before adding SiC particles. The composite melt was cooled into a permanent die. Figure 1a–c exhibited the aluminium stir casting furnace (100 kg capacity), die-casted specimen (finger form), and pin specimen after machining for abrasive wear testing, respectively. For T6 heat treatment, the as-cast samples were solutionised at 495 °C for 8 h and then quenched in oil at room temperature; after that, artificial ageing was done at 175 °C for 6 h, and finally, the aged samples were cooled in ambient air Ref. [37].

2.2 Microstructural Studies

The morphological characterisation of fresh abrasive papers, alloys, and composite was done under FESEM (Ultra Plus, Carl Zeiss Microscopy GmbH, Oberkochen, Germany), and morphology of SiC reinforcement was characterised by SEM (5600, JEOL Ltd., Akishima, Tokyo, Japan). Before morphological examinations, the specimens of alloys and composite were metallographically polished and then etched by using Keller's reagent. The wear surface, abrasive paper after abrasive wear tests, and wear debris particles were analysed by FESEM.

2.3 Measurements of Density and Hardness

The density measurements of alloys and composite were carried out by density kit (WDK250, Wensar Weighing Scales Limited, Chennai, India) with the precision of 0.0001 g and which is adopted the water displacement technique. The three density values were obtained, and the mean value was represented. The hardness measurements of as-cast and heat-treated alloys and composite were carried out by a Vickers hardness tester. The specimen surface was polished, and the backside of the specimen surface was made flat. The measurements of the specimens were done at 5 kgf of the applied load and 5 s dwell time. The five hardness values were obtained, and the mean value was represented.

2.4 High-Stress Abrasive Wear Test

The wear examination was conducted on metallographically polished (length: 30 mm, diameter: 10 mm) cylindrical pins using a pin-on-disk tribometer (TR20-LE, Ducom Instruments, Bangalore, India). The parameters such as 5–20 N applied load, 100–400 m abrading distance (sliding distance), 38–80 μm self-adhesive SiC abrasive paper size, 1 m/s fixed sliding speed of and 100 mm track diameter. The self-adhesive SiC abrasive papers of the desired size were pasted on a wheel (Ø50 mm × 12 mm (t)) to act as the abrasive media. Before and after the test, the specimen was cleaned by using acetone and weighed with the microbalance. The mass loss of tested samples was changed into a volume loss, which was used to calculate the wear rate of samples. A detailed explanation of the wear test was given in Ref. [37].

Fig. 1 The image of **a** stir casting furnace **b** die-casted specimen (finger form) **c** pin specimen after machining for abrasive wear testing
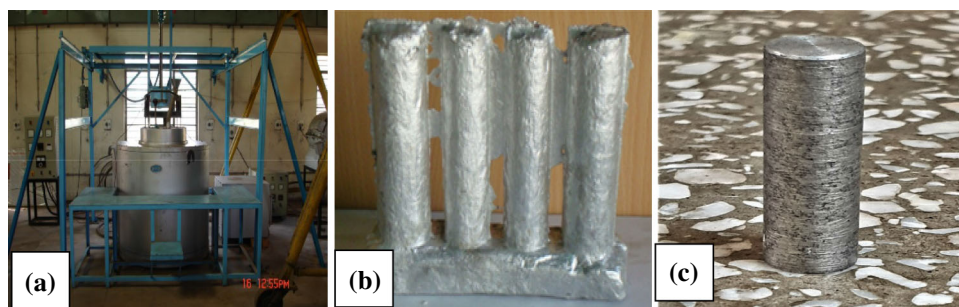
3 Results and Discussion

3.1 Microstructural Analysis

Figure 2a exhibited the nature of particles that was equiaxed and sharp-edged [36]. The morphology of fresh abrasive paper size of 38–80 μm was shown in Fig. 2b–e. These figures clearly showed the orientation, cutting edge, angular shape, and the tip of the abrasive particles. The microstructure of the as-cast LM25 alloy, LM30 alloy, and LM25-SiC composite was exhibited in Fig. 2f–h. The microstructure of LM25 alloy was showed the significant breakup of the plate or sharp edged-shaped eutectic silicon particles and aluminium dendrites. The microstructure of the LM30 alloy shows the primary Si and Al-Si eutectic phases. The microstructure of the LM25-SiC composite showed the homogeneous dispersion of SiCp in the matrix and excellent bonding of the Al matrix and SiC interface. The effect of T6 heat-treatment on the microstructure of alloys and composite explanation is given in Ref. [37].

3.2 Analysis of Density and Hardness

The density of LM25 alloy, hypereutectic alloy, and composite was found to be 2.6701 ± 0.0015, 2.7132 ± 0.0027, and 2.7311 ± 0.0014 g/cm^3, respectively. The composite showed higher density as compared to LM25 alloy and hypereutectic (LM30) alloy because of the addition of SiC particles. The hardness mean values of the as-cast LM25 alloy, hypereutectic (LM30) alloy, and composite was found to be 75 ± 2, 103 ± 3, and 149 ± 2 Hv, respectively, which was improved by 28%, 21%, and 9% after the heat treatment. This improvement was caused by the formation of intermetallic precipitates [37].

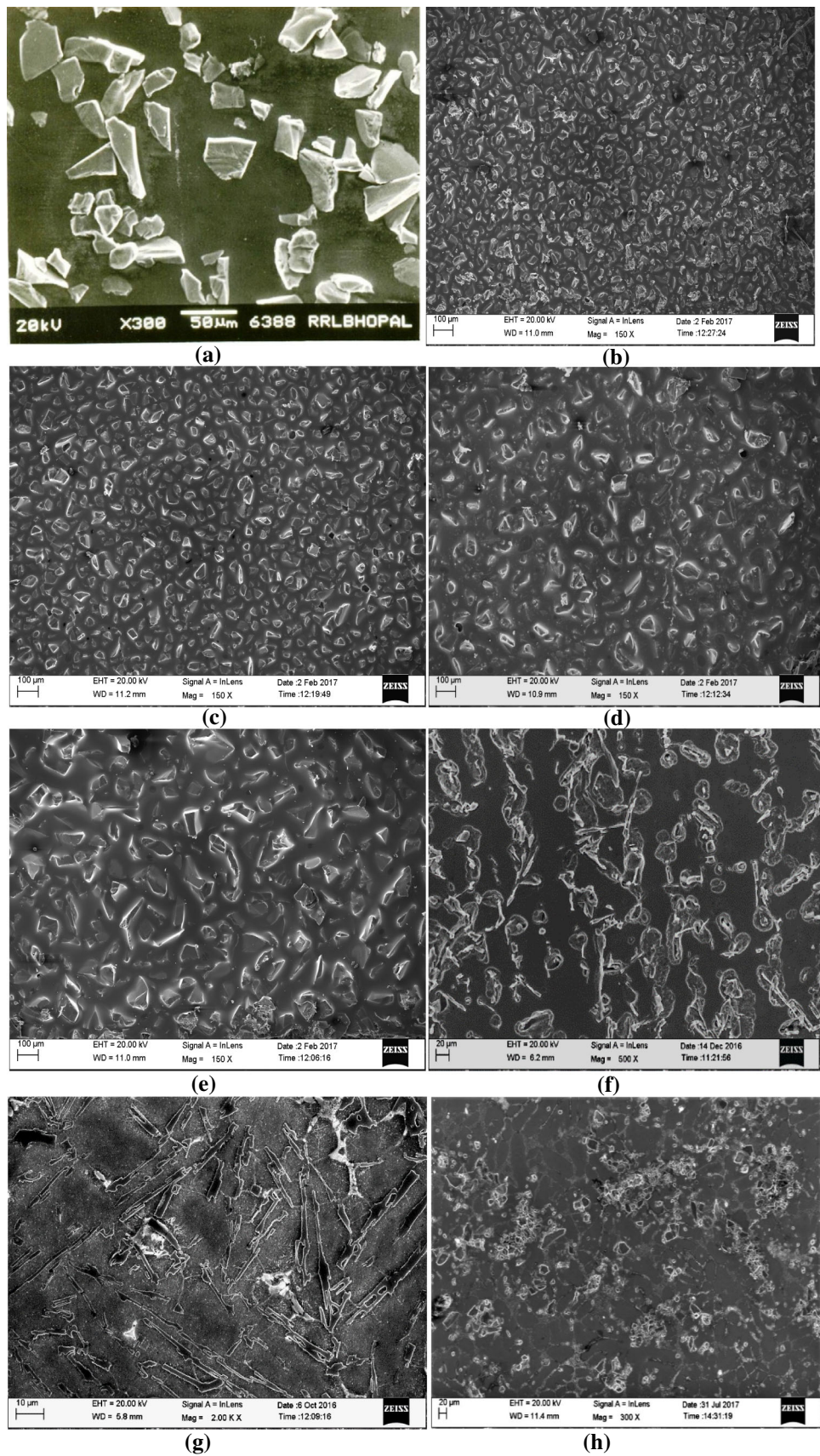### 3.3 Abrasive Wear Rate as a Function of Abrasive Size

The high-stress abrasive wear rate of the materials in as-cast and after T6 heat treatment was shown in Fig. 3a–d in terms of abrasive size at varying applied load and 400 m abrading distance. The abrasive wear rate of LM30 alloy and LM25-SiC composite as compared to the base value of LM25 alloy in the influence of abrasive (grit) size.

Figure 3a exhibited that at 5 N applied load and 38 μm abrasive size, the abrasive wear rate of as-cast LM25 alloy, LM30 alloy, and LM25-SiC composite was found 0.02397 mm^3/m, 0.01456 mm^3/m, and 0.00218 mm^3/m, respectively and for 80 μm abrasive size, the wear rate was 0.15114 mm^3/m, 0.05368 mm^3/m, and 0.00673 mm^3/m, respectively. The wear rate was decreased 39.26% and 90.91% at 38 μm abrasive size, and for 80 μm abrasive size, the wear rate was reduced 64.48% and 95.55% for LM30 alloy and LM25-SiC composite, respectively. Figure 3b exhibited that, at 5 N applied load and 38 μm abrasive size, the wear rate of heat-treated LM25 alloy, LM30 alloy, and LM25-SiC composite were 0.02071 mm^3/m, 0.01275 mm^3/m and 0.00147 mm^3/m, respectively and for 80 μm abrasive size, the wear rates were 0.05866 mm^3/m, 0.01856 mm^3/m, and 0.00576 mm^3/m, respectively. The wear rate was decreased 38.44% and 92.90% at 38 μm abrasive size, and for 80 μm abrasive size, the wear rate was reduced 68.36% and 90.18% for LM30 alloy and LM25-SiC composite, respectively. Figure 3c exhibited that, at 20 N applied load and 38 μm abrasive size, the wear rate of as-cast LM25 alloy, LM30 alloy, and LM25-SiC composite was found to be 0.13069 mm^3/m, 0.09641 mm^3/m, and 0.00892 mm^3/m, respectively and for 80 μm abrasive sizes of the wear rate were 0.75889 mm^3/m, 0.51742 mm^3/m, and 0.03512 mm^3/m, respectively. The wear rate was decreased 26.23% and 93.17% at 38 μm abrasive sizes, and for 80 μm abrasive size, the wear rate was reduced 31.82% and 95.37% for LM30 alloy and LM25-SiC composite, respectively. Figure 3d exhibited that, at 20 N applied load and 38 μm abrasive size, the wear rate of heat-treated LM25 alloy, LM30 alloy, and LM25-SiC composite were 0.10912 mm^3/m, 0.06593 mm^3/m, and 0.00722 mm^3/m, respectively and for 80 μm abrasive size, the wear rate was found to be 0.61072 mm^3/m, 0.41147 mm^3/m, and 0.02069 mm^3/m, respectively. The wear rate was decreased 39.58% and 93.38% at 38 μm abrasive size, and for 80 μm abrasive size, the wear rate was reduced 32.63% and 96.61% for LM30 alloy and LM25-SiC composite, respectively.

At 5 N applied load, after heat treatment of LM25 alloy, LM30 alloy, and LM25-SiC composite, the percentage of

Fig. 2 **a** Morphology of SiC reinforcement [36], Morphology of silicon carbide abrasive paper of the abrasive size of **b** 38 µm **c** 46 µm **d** 60 µm **e** 80 µm, and microstructure of **f** LM25 alloy **g** LM30 alloy **h** LM25-10%SiC composite
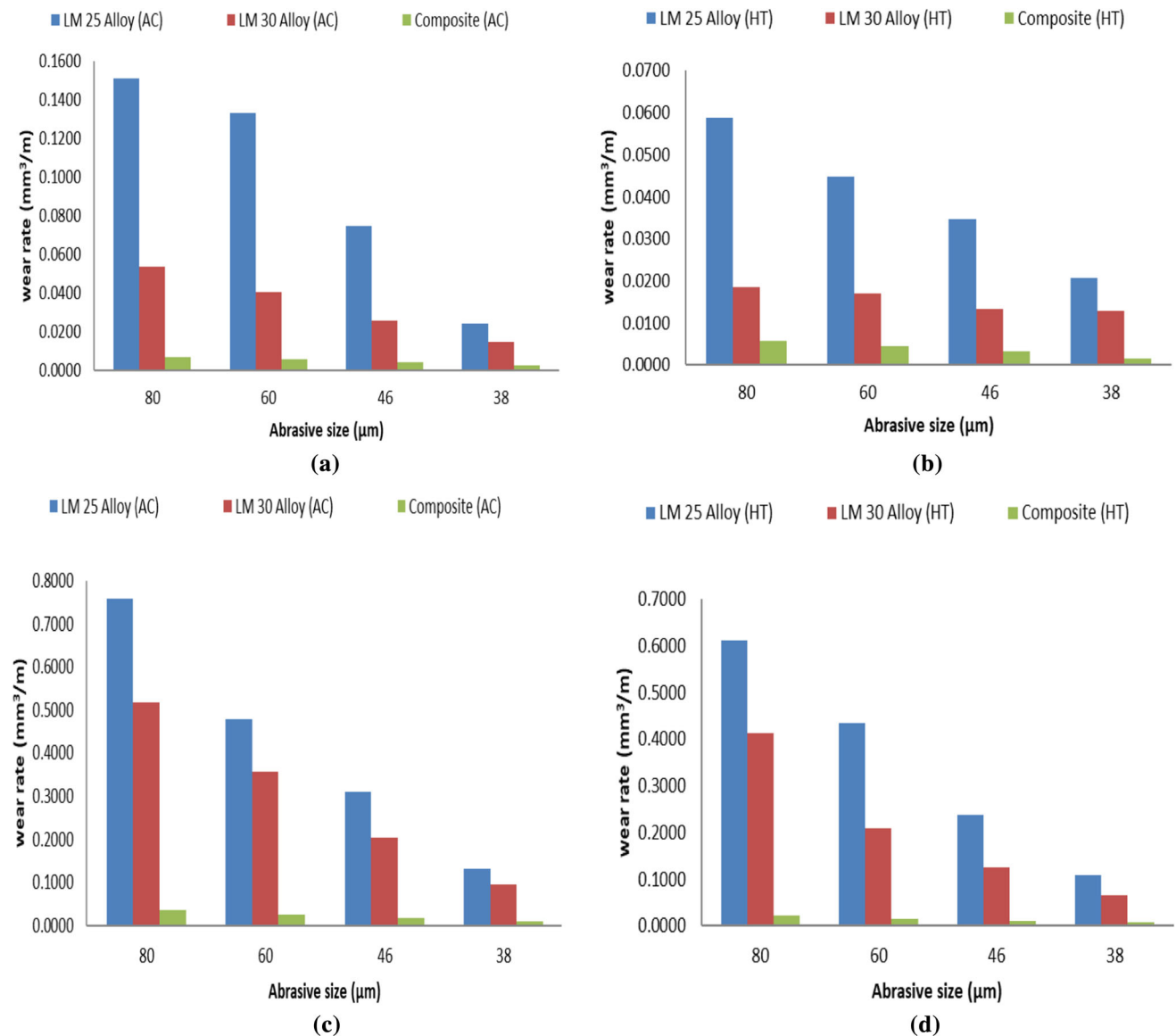
Fig. 3 Wear rate of the materials as a function of the abrasive size at the sliding distance of 400 m, **a**, **c** 5 N and 20 N in as-cast (AC) condition and **b**, **d** 5 N and 20 N in the heat-treated (HT) condition

wear rate was decreased 13.60, 12.43 and 32.57, respectively at 38 µm abrasive size, and 61.19, 65.42, and 14.41 in case of 80 µm abrasive size, respectively. However, at 20 N applied load, the percentage of wear rate was decreased 16.50, 31.61, and 19.06, respectively at 38 µm abrasive size, and 19.52, 20.48, and 41.09, respectively for the 80 µm abrasive size. It is observed that the depth of penetration into the specimen increases with the increase in the abrasive (grit) sizes; consequently, the wear rate increases for both as-cast and heat-treated conditions [38–40]. It was noticed that the addition of SiC reinforcement to matrix alloy enhanced the wear resistance of the matrix hypoeutectic alloy and hypereutectic alloy in both the as-cast and heat-treatment conditions. The wear resistance of the heat-treated speci-

mens was improved than the as-cast specimens due to the formation of smooth-edged (spherical) silicon particles and intermetallic precipitations of other alloying elements (such as Mg, Cu, Fe Mn, and Ni) in the materials; this leads to more strength and toughness of the heat-treated materials [33, 40–42]. As the abrasive size increases, the wear resistance of as-cast and heat-treated LM30 alloy was found to be superior to the matrix alloy but inferior to the composite. LM25 is a hypoeutectic alloy in which eutectic silicon was appeared needle-shaped. On the other hand, hypereutectic alloy (LM30) primary silicon was showed as a cuboid, and needle-shaped eutectic silicon was also discernable (Fig. 2). The needle-shaped sharp-edged eutectic silicon resulted in higher stress concentration, and during the wear test, the

applied load initiated crack nucleation and then propagation of crack-formed wear debris. In LM30 alloy, the primary cuboid-shaped silicon, of size around 20 μm, resisted wear of material and showed better wear resistance than LM25 alloy. Additionally, in LM30 alloy, there was no primary soft aluminium, and the entire matrix consisted of eutectic silicon, which resisted further wear of the material. In the case of LM25-SiC particle composite, the dispersed SiC hard particles (around 20–40 μm in size) protruded the wear surface and enhanced the wear resistance. SiC particles were much harder than primary silicon and showed better wear resistance both in as-cast and heat-treated conditions.

3.4 Analysis of Wear Surfaces

3.4.1 Specimen

The wear (abraded) surface of specimens in the as-cast condition was analysed by using FESEM to unveil the wear mechanism, as shown in Fig. 4. Figure 4a and c indicated the abraded surfaces of LM25 alloy and LM30 alloy at 38 μm abrasive size and 5 N applied load, respectively. Abrasive paper embedded with SiC particles penetrated the soft material of matrix alloy and hypereutectic alloy. During reciprocation, hard SiC particles ploughed the specimen surface by removing the soft materials into the ridge along the side of the grooves. The wear surface of the alloys revealed that long continuous grooves were formed during abrasion, and cracks propagating in the direction of longitudinal and transverse. Figures 4b and d exhibited the wear surface of LM25 alloy and LM30 alloy at 80 μm abrasive size and 20 N applied load, respectively. The wear surface features a long continuous groove and some plastically damaged regions. These surfaces also exhibited that the width and depth of the grooves were slightly bigger than those shown in Fig. 4a and c. The width and depth of the grooves on the wear surface depend upon the abrading action of the hard particles of the wear debris. Further, the severity of damage of the material surface increased with the abrasive size and applied load (Fig. 4b versus a, and Fig. 4d versus c). Figure 4e–f exhibited the wear surface of the composite at 38, and 80 μm abrasive size and 5 and 20 N applied load, respectively. Figure 4e exhibited silicon carbide particles (hard dispersoid) sticking out from the abrading surface of the composite. These particles were stable and intact within the matrix of the composite. The interfacial strength of the particle with the matrix was weakened; consequently, the matrix of the composite during abrasion allows smaller particles to get released from it (marked by the arrow). The wear surface of the composite also showed a finer and smoother wear track compared to both alloys. Figure 4f indicated the large flakes of the matrix (because of fracture), voids(due to the coming out of dispersoids from the matrix), and a heap of dispersoids in the wear

surface of the composite. For larger abrasive size and applied load, the materials were displaced due to micro-fatigue cracking, ploughing, and cutting. As a result, the silicon carbides particle was revealed in the primary stage. Subsequently, at a long abrading distance, this SiC particle was fragmented as well as scooped off from the abrading surface. Hence it was analysed that the LM25-SiC composite was superior wear resistance (less surface damage) as compared to the matrix alloy and hypereutectic alloy. The wear surface of the heat-treated materials was found to be similar wear surface mechanism as observed to that of as-cast ones.

3.4.2 Abrasive Paper

The wear surface of the abrasive papers (emery papers) at the different abrasive sizes and applied loads were shown in Fig. 5. Figure 5a, c, and e exhibited the abrasive paper after abrading the LM25 alloy, LM30 alloy, and LM25-SiC composite at 38 μm abrasive sizes, and 5 N applied load, respectively. However, Figs. 5b, d, and f showed the abrasive paper after abrading the LM25 alloy, LM30 alloy, and LM25-SiC composite at 80 μm abrasive size and 20 N applied load, respectively. The inter (abrasive) particle spacing of finer size of abrasive paper (5a, c and e) was significantly less than the coarser size of abrasive paper (5b, d and f). Entrapment of the wear debris on the abrasive paper of both alloys was relatively more than the composite because alloys have higher ductility. The wear debris consisted of machining chips, flakes, and fragmented particles. The size and quantity of the wear debris became greater when the applied load was increased (Fig. 5b, d and f versus Fig. 5a, c and e, respectively). Fracturing, microcracking, and removal of the abrasive particles (degraded) of the abrasive paper were observed in Fig. 5. For alloys, the region of protrusion of the degraded abrasive medium on the abrasive paper surface became less, whereas fracture/removal of abrasive particles improved with abrading distance. In the case of composite, the region of protrusion of the degraded abrasive medium on the abrasive paper surface decreased with abrading distance and applied load [43].

Abrasive particles were subjected to subsurface work hardening, fragmentation/removal of the hard (dispersoid) phase, capping (wear debris covered the tip of the abrasive particles), attrition (blunting of the tip/cutting edge of the abrasive particles), shelling (abrasive particle removal due to microcracking/damage) and clogging (debris get entrapped between the inter (abrasive) particles spacing), during abrasion process. The degree of capping, clogging, shelling, and attrition increased with increasing the applied load (Fig. 5b, d and f versus Fig. 5a, c and e, respectively) and abrading distance. The degree of capping and clogging decreased while shelling and attrition increased when the specimen surface being abraded contains hard reinforcement particles. Generally, capping, clogging, shelling, and attrition decreased

Fig. 4 Wear surface analysis of specimens **a** LM25 alloy at 38 μm abrasive size, and 5 N applied load **b** LM25 alloy at 80 μm abrasive size, and 20 N applied load **c** LM30 alloy at 38 μm abrasive size, and 5 N applied load **d** LM30 alloy at 80 μm abrasive size, and 20 N applied load **e** LM25-SiC composite at 38 μm abrasive size, and 5 N applied load **f** LM25-SiC composite 80 μm abrasive size and at 20 N applied load
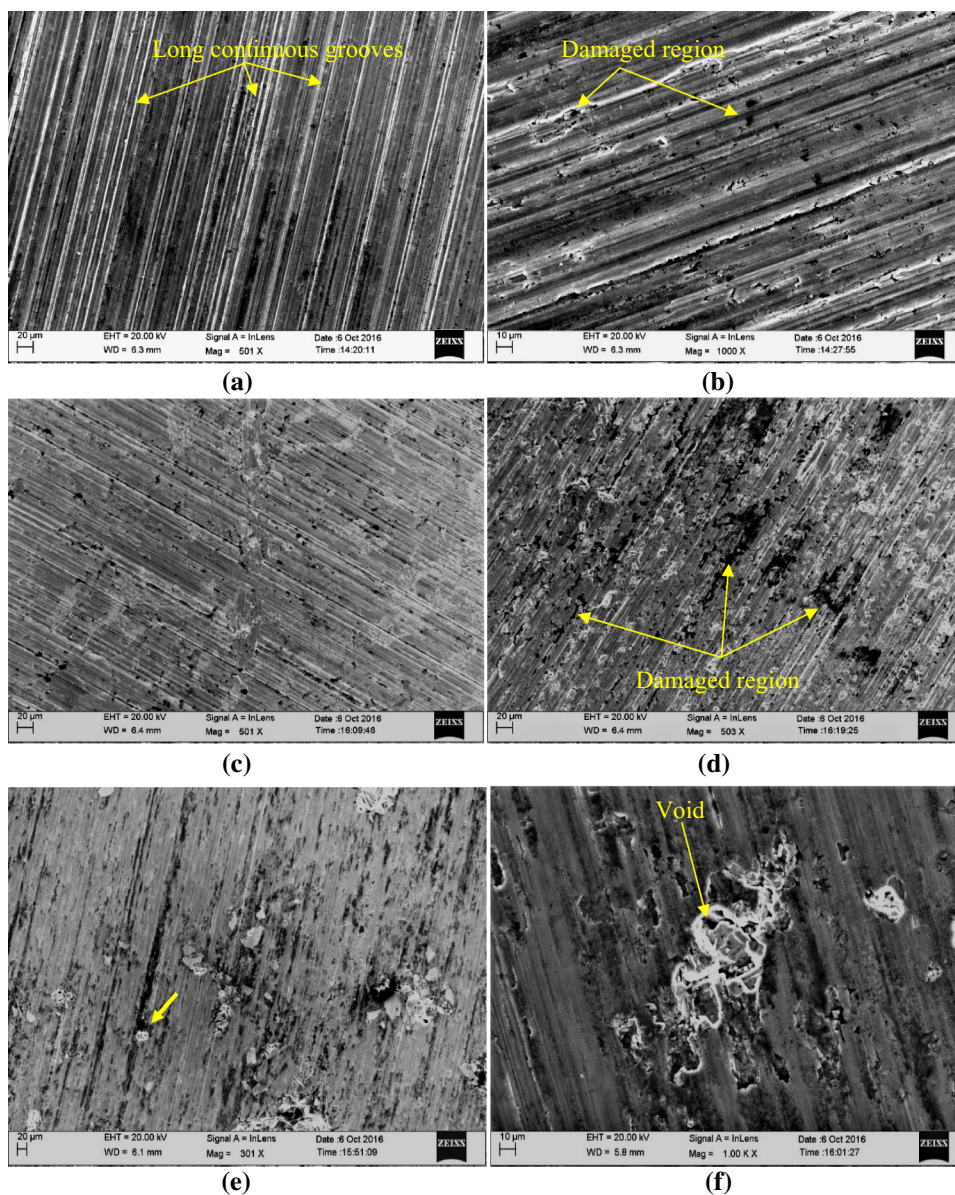

the cutting efficiency of the abrasives, due to which reduction in wear rate. The effect of several parameters shows that diminution in cutting efficiency of abrasives (by capping, clogging, shelling, and attrition), the wear resistance produced by dispersoid (SiC) particle and subsurface work hardening of the matrix leading to more excellent wear resistance (i.e. lower wear rate) in case of composite, however fragmentation/removal of the hard dispersoid phase would have a reverse effect in case of alloys [44, 45].

3.5 Wear Debris

Figure 6 showed the wear debris of specimens at the different abrasive sizes and applied loads in as-cast conditions to unveil the wear mechanism. The wear debris of LM25 alloy, LM30 alloy, and LM25-SiC composite for 38 μm abrasive size and 5 N applied load was exhibited in Fig. 6a, (c) and (e), respectively. Meanwhile, the wear debris of LM25 alloy, LM30 alloy, and LM25-SiC composite for 80 μm abrasive size and 20 N applied load was exhibited in Fig. 6b, d and f, respectively.

Fig. 5 Wear surface analysis of abrasive paper **a** LM25 alloy at 38 μm abrasive size, and 5 N applied load **b** LM25 alloy at 80 μm abrasive size, and 20 N applied load **c** LM30 alloy at 38 μm abrasive size, and 5 N applied load **d** LM30 alloy at 80 μm abrasive size, and 20 N applied load **e** LM25-SiC composite at 38 μm abrasive size, and 5 N applied load **f** LM25-SiC composite 80 μm abrasive size and at 20 N applied load
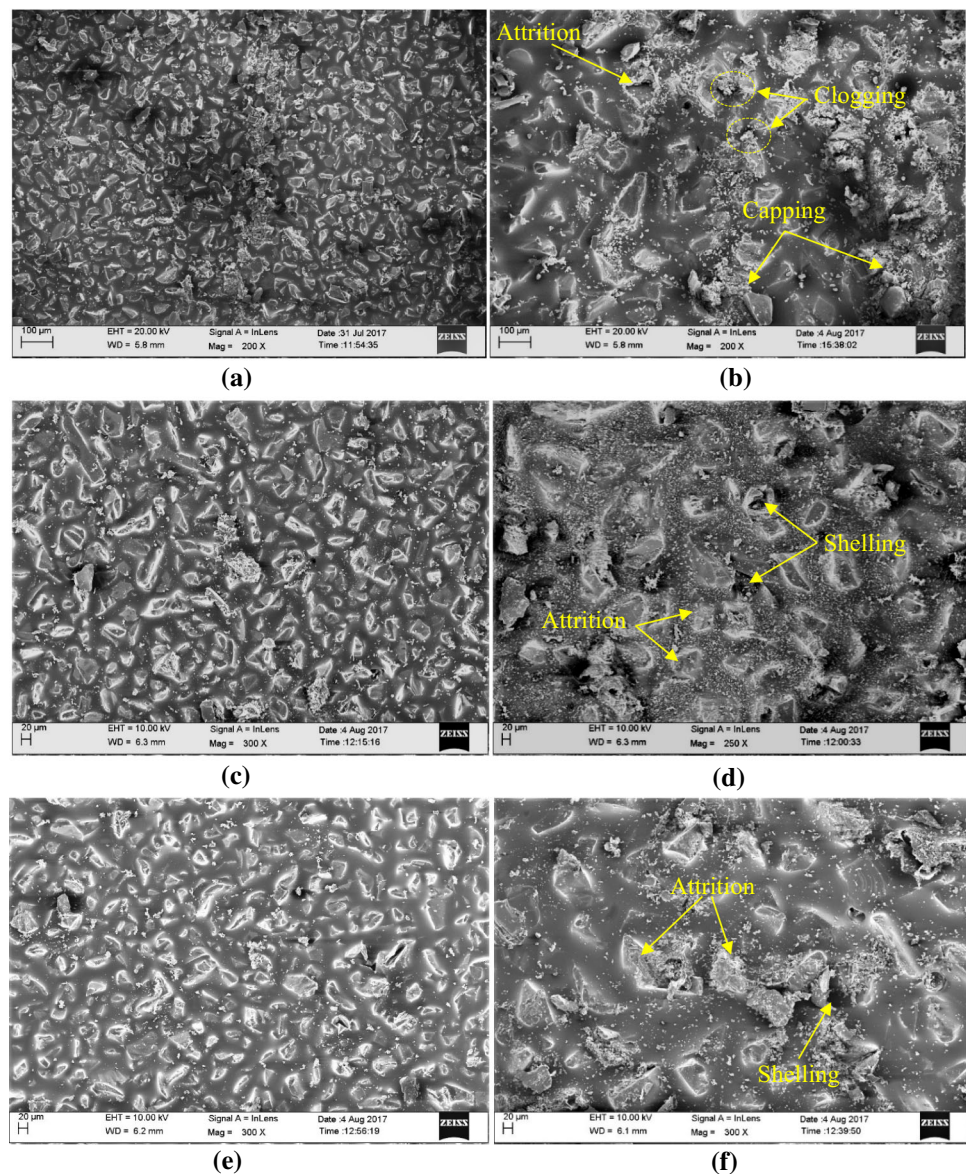
The responsible parameter for the penetration depth of abrasive particles relies on the rake angle (attack angle) of the tip of the abrasive particle [45–47], the degree of contact stresses between the pin surface and abrasive medium [43], the hardness of pin surface [47, 48] and the abrasive size of the medium [45, 47–49]. Microcutting (Machining) chips were formed by cutting edge/tip of the abrasive particle, which cut the pin surface at a higher rake angle (attack angle), whereas warped flakes were formed by the cutting edge of the abrasive, which cut the surface at lower attack angle [46]. The depth of penetration increases with the applied load, abrasive size of the medium, and rake angle, and also increased the wear rate. However, the depth of penetration decreased with an increase in the hardness of the pin surface. As a result, at the higher abrasive size and applied load, the specimens expe-

rienced more wear rate as exhibited in Fig. 3a–d and broader and longer flakes, which were exhibited in Fig. 6. In the case of alloys, most of the debris was comprised of warped flakes and macrocutting (machining) chips. Fractured/fragmented abrasive particles of the abrasive medium were also noted in wear debris. For the composite, wear debris comprised of discontinuous macrocutting chips and warped flakes, as well as fractured dispersoid particles [43]. The size of wear debris increased with an applied load while increasing the size of abrasive, debris became coarser irrespective of the materials. The degree of a generation of flakes was more at the greater applied load and coarser abrasive size irrespective of the materials because penetration depth on the pin surface was more. More damage in pin surface, the formation of coarser debris, and less attrition capping, and clogging of

Fig. 6 Wear debris analysis of
a LM25 alloy at 38 μm abrasive
size, and 5 N applied load
b LM25 alloy at 80 μm abrasive
size, and 20 N applied load
c LM30 alloy at 38 μm abrasive
size, and 5 N applied load
d LM30 alloy at 80 μm abrasive
size, and 20 N applied load
e LM25-SiC composite at
38 μm abrasive size, and 5 N
applied load **f** LM25-SiC
composite 80 μm abrasive size
and at 20 N applied load
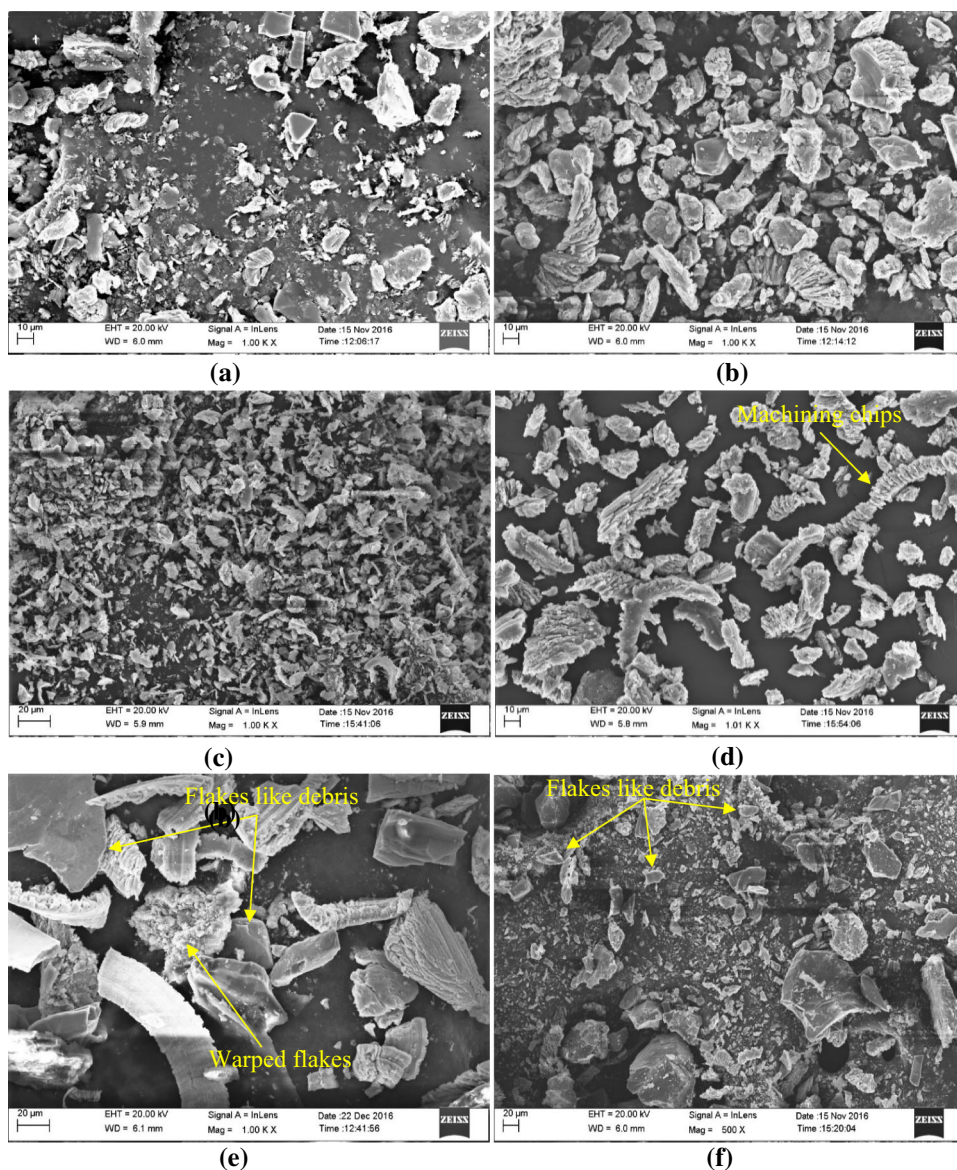
the abrasives led to a greater wear rate and vice versa [43]. The wear debris of the heat-treated materials was found to be similar wear debris mechanism as observed to as-cast ones. It was presumed that hypereutectic Al-Si (LM30) alloy would be a suitable material for wear resistance application compared to LM25-SiC composites. However, the wear-resistant properties evaluated in the present investigation depicted that LM25-SiC composite showed higher wear resistance properties than LM30 alloy. The dispersion of 10 wt%, 10–20 μm size SiC particles in LM25 alloy enhanced the wear properties substantially compared to LM30 alloy. These composites are proved to be ideal materials for automobile components like connecting rods and other components where wear resistance is a prime consideration.

4 Conclusion

The results of the investigations can be summarised as follows:

1. The composite was a higher density and hardness than the LM25 alloy and LM30 alloy

   a. because of the presence of SiC particles. The hardness of matrix alloy, hypereutectic alloy, and composite was improved after the heat treatment because of the formation of intermetallic precipitates.

2. The abrasive wear resistance of composite was excellent compared to the matrix alloy and hypereutectic alloy in both as-cast and after heat-treatment, by the presence of

SiCp to the base alloy. Additionally, the abrasive wear resistance of hypereutectic alloy was improved than the matrix alloy because of more wt% of silicon content.

3. For coarser abrasive size and higher applied load, the decrement in abrasive wear rate of LM30 alloy and LM25-SiC composite was 31.82% and 95.37%, respectively, in the case of the as-cast condition. However, for heat-treated conditions, the decrement in wear rate of LM30 alloy and LM25-SiC composite was 32.63% and 96.61%, respectively.

4. At the finer abrasive size and lower applied load, the width and depth of the groove of the materials in both as-cast and after heat-treatment were slightly smaller than the coarser abrasive size and greater applied load. The wear surface of the LM25-SiC composite shows shallow scratches, finer and smoother wear track compared to both alloys.

5. The wear surface of abrasive paper exhibits the fracturing, microcracking, and removal of the abrasive particles (degraded) in some regions.

6. The influence of abrasive size had a greater effect on the wear rate, which can be seen in the material removal mechanism and abrasive wear surface. The abrasive wear rate of the specimen increased with an increase in the abrasive size caused by an increase in material removal ability. For coarser abrasive size and higher load, penetration depth would be more; consequently, the materials were displaced due to micro-fatigue cracking, ploughing, and cutting.

Declarations

Conflict of interest The authors declared that there is no conflict of interest.

References

1. Miller, W.S.; Zhuang, L.; Bottema, J.; Wittebrood, A.J.; Smet, P.D.; Haszler, A.; Vieregge, A.: Recent development in aluminium alloys for the automotive industry. Mater. Sci. Eng. A **280**, 37–49 (2000). https://doi.org/10.1016/S0921-5093(99)00653-X

2. Brown, K.R.; Venie, M.S.; Woods, R.A.: The increasing use of aluminium in automotive applications. JOM **47**, 20–23 (1995). https://doi.org/10.1007/BF03221224

3. Lloyd, D.J.: Particle reinforced aluminium and magnesium matrix composites. Int. Mater. Rev. (1994). https://doi.org/10.1179/imr.1994.39.1.1

4. Rohatgi, P.K.: Cast aluminium-matrix composites for automotive applications. JOM **43**, 10–15 (1991). https://doi.org/10.1007/BF03220538

5. Yoshimuro, H.N.; Goncalves, M.C.; Goldenstein, H.: The effect of SiCp clusters and porosity on the mechanical properties of PM Al matrix composites. Key Eng. Mater. **127–131**, 985–992 (1997)

6. Zeuner, T.; Stojanov, P.; Sahm, P.R.; Ruppert, H.; Engels, A.: Developing trends in disc brake technology for rail application. Mater. Sci. Technol. **14**, 857–863 (1998)

7. Günay, M., Şeker, U.: Evaluation of Surface Integrity during Machining with Different Tool Grades of Sicp/Al-Si Composites Produced by Powder Metallurgy. Mater. Sci. Forum. 319–322 (2011)

8. Wang, D.; Zhang, H.; Nagaumi, H.; Jia, P.; Cui, J.: Microstructural homogeneity, mechanicalproperties, and wear behavior of in situ Mg_2Si particles reinforced Al–matrix composites fabricated by hot rolling. J. Mater. Res. Technol. **9**, 1882–1892 (2019)

9. Alizadeh, A.; Taheri-Nassaj, E.: Mechanical properties and wear behavior of Al–2wt. %Cu alloy composites reinforced by B4C nanoparticles and fabricated by mechanical milling and hot extrusion. Mater. Charact. **67**, 119–128 (2012). https://doi.org/10.1016/j.matchar.2012.02.006

10. Vencl, A.; Bobic, I.; Arostegui, S.; Bobic, B.; Marinković, A.; Babić, M.: Structural, mechanical and tribological properties of A356 aluminium alloy reinforced with Al_2O_3, SiC and SiC + graphite particles. J. Alloys Compd. **506**, 631–639 (2010)

11. Abdizadeh, H.; Baghchesara, M.A.: Investigation on mechanical properties and fracture behavior of A356 aluminum alloy based ZrO_2 particle reinforced metal-matrix composites. Ceram. Int. **39**, 2045–2050 (2013). https://doi.org/10.1016/j.ceramint.2012.08.057

12. Das, S.: Development of aluminium alloy composites for engineering applications. Trans. Indian I. Met. **57**, 325–334 (2004)

13. Surappa, M.K.: Aluminium matrix composites: challenges and opportunities. Sadhana (2003). https://doi.org/10.1007/BF02717141

14. Das, S.; Mondal, D.P.; Modi, O.P.; Dasgupta, R.: Influence of experimental parameters on the Erosive-corrosive wear of Al–SiC particle composite. Wear **231**, 195–205 (1999)

15. Prasad, S.V.; Asthana, R.: Aluminium metal-matrix composites for automotive applications: tribology considerations. Tribol. Lett. **17**, 445–453 (2004)

16. Ahlatci, H.; Cimenoglu, H.; Candan, E.: Mechanical properties of Al–60% SiCp composites alloyed with Mg. Metall. Mater. Trans. A **35**, 2127–2141 (2004)

17. Rohatgi, P.K.: Metal matrix composites. Adv. Mater. Technol. Monitor **17**, 1–47 (1990)

18. Roy, M.; Venkataraman, B.; Bhanuprasad, V.; Mahajan, Y.; Sundararajan, G.: The effect of particulate reinforcement on the sliding wear behaviour of aluminium matrix composites. Metall. Trans. A **23**, 2833–2847 (1992). https://doi.org/10.1007/BF02651761

19. Natarajan, N.; Vijayarangan, S.; Rajendran, I.: Wear behaviour of A356/25SiCp aluminium matrix composites sliding against automobile friction material. Wear **261**, 812–822 (2006)

20. Surappa, M.K.: Dry sliding wear of fly ash particle reinforced A356 Al composites. Wear **265**(3–4), 349–360 (2008)

21. Kucukomeroglu, T.: Effect of equal-channel angular extrusion on mechanical and wear Properties of eutectic Al–12Si alloy. Mater. Des. **31**, 782–789 (2010)

22. Shivamurthy, R.C.; Surappa, M.K.: Tribological characteristics of A356 Al alloy–SiCp composite discs. Wear **271**, 1946–1950 (2011). https://doi.org/10.1016/j.wear.2011.01.075

23. Toptan, F.; Kerti, I.; Rocha, L.A.: Reciprocal dry sliding wear behaviour of B4Cp reinforced aluminium alloy matrix composites. Wear **290–291**, 74–85 (2012)

24. Feyzullahoglu, E.; Ertürk, A.T.; Güven, E.A.: Influence of forging and heat treatment on wear properties of Al-Si and Al-Pb bearing alloys in oil lubricated conditions. T. Nonferr.

Metal. Soc. **23**, 3575–3583 (2013). https://doi.org/10.1016/S1003-6326(13)62903-9

25. Zhang, S.; Dong, X.; Zhao, Y.; Liu, M.; Chen, G.; Zhang, Z.; Zhang, Y.; Gao, X.: Preparation and wear properties of TiB$_2$/Al−30Si composites via in-situ melt reactions under high-energy ultrasonic field. T. Nonferr. Metal. Soc. **24**, 3894–3900 (2014)

26. Khosravi, H.; Akhlaghi, F.: Comparison of microstructure and wear resistance of A356−SiCp composites processed via compocasting and vibrating cooling slope. T. Nonferr. Metal. Soc. **25**, 2490–2498 (2015). https://doi.org/10.1016/S1003-6326(15)63867-5

27. Mosleh-Shirazi, S.; Akhlaghi, F.; Li, D.Y.: Effect of SiC content on dry sliding wear, corrosion and corrosive wear of Al/SiC nanocomposites. T. Nonferr. Metal. Soc. **26**, 1801–1808 (2016). https://doi.org/10.1016/S1003-6326(16)64294-2

28. Pitchayyapillai, G.; Seenikannan, P.; Balasundar, P.; Narayanasamy, P.: Effect of nano-silver on microstructure, mechanical and tribological properties of cast 6061 aluminium alloy. T. Nonferr. Metal. Soc. **27**, 2137–2145 (2017). https://doi.org/10.1016/S1003-6326(17)60239-5

29. Lakshmikanthan, A.; Bontha, S.; Krishna, M.; Koppad, P.G.; Ramprabhu, T.: Microstructure, mechanical and wear properties of the A357 composites reinforced with dual sized SiC particles. J. Alloys compd. **786**, 570–580 (2019). https://doi.org/10.1016/j.jallcom.2019.01.382

30. Kumar, H.; Prasad, R.; Kumar, P.; Tewari, S.P.; Singh, J.K.: Mechanical and tribological characterisation of industrial wastes reinforced aluminium alloy composites fabricated via friction stir processing. J. Alloys Compd. (2020). https://doi.org/10.1016/j.jallcom.2020.154832

31. Sahin, Y.: Wear behaviour of aluminium alloy and its composites reinforced by SiC particles using statistical analysis. Mater. Des. **24**, 95–103 (2003)

32. Sahin, Y.: Optimisation of testing parameters on the wear behaviour of metal matrix composites based on the Taguchi method. Mater. Sci. Eng. A **408**, 1–8 (2005)

33. Sahin, Y.: Abrasive wear behaviour of SiC/2014 aluminium composite. Tribol. Int. **43**, 939–943 (2010). https://doi.org/10.1016/j.triboint.2009.12.056

34. Mondal, D.P.; Das, S.: High-stress abrasive wear behaviour of aluminium hard particle composites: Effect of experimental parameters, particle size and volume fraction. Tribol. Int. **39**, 470–478 (2006). https://doi.org/10.1016/j.triboint.2005.03.003

35. Sharma, R.; Anesh, D.: DK. Solutionizing temperature and abrasive wear behaviour of cast Al–Si–Mg alloys. Mater Des **28**, 1975–1981 (2007)

36. Shah, K.B.; Kumar, S.; Dwivedi, D.K.: Aging temperature and abrasive wear behaviour of cast Al–(4%, 12%, 20%) Si–0.3% Mg alloys. Materials & design **28**(6), 1968–1974 (2007)

37. Singh, R.K.; Telang, A.; Das, S.: Microstructure, mechanical properties and two-body abrasive wear behaviour of hypereutectic Al−Si−SiC composite. T. Nonferr. Metal. Soc. **30**, 65–75 (2020). https://doi.org/10.1016/S1003-6326(19)65180-0

38. Singh, R.K.; Telang, A.; Das, S.: Microstructure, mechanical, and high-stress abrasive wear behaviour of as-cast and heat-treated Al–Si–SiCp composite. Int. J. Mater. Res. **110**, 121–129 (2019). https://doi.org/10.3139/146.111727

39. Sahin, Y.; Ozdin, K.: A model for the abrasive wear behaviour of aluminium based composites. Mater. Des. **29**, 728–733 (2008). https://doi.org/10.1016/j.matdes.2007.02.013

40. Wang, A.G.; Hutchings, I.M.: Wear of alumina fibre-aluminium metal matrix composites by two-body abrasion. Mater. Sci. Technol. **5**, 71–76 (1989)

41. Das, S.; Mondal, D.P.; Sawla, S.; Ramakrishnan, N.: Synergic effect of reinforcement and heat treatment on the two-body abrasive wear of an Al-Si alloy under varying loads and abrasive sizes. Wear **264**, 47–59 (2008). https://doi.org/10.1016/j.wear.2007.01.039

42. Lin, S.; Liu, K.: Effect of aging on abrasion rate in an Al-Zn-Mg-SiC composite. Wear **121**, 1–14 (1988). https://doi.org/10.1016/0043-1648(88)90026-9

43. Zongyi, M.; Jing, B.; Yuxiong, L.; Hongwei, S.; Yinxuan, G.: Abrasive wear of discontinuous SiC reinforced aluminium alloy composites. Wear **148**, 287–293 (1991)

44. Prasad, B.K.: Abrasive wear characteristics of a zinc-based alloy and zinc-alloy/SiC composite. Wear **252**, 250–263 (2002). https://doi.org/10.1016/S0043-1648(01)00872-9

45. Prasad, B.K.; Das, S.: Abrasive wear characteristics of Zn–37.2 Al–2.5 Cu–0.2 Mg alloy dispersed with silicon carbide particles. Mater. Trans. JIM **36**(8), 1048–1057 (1995)

46. Prasad, B.K.; Das, S.; Jha, A.K.; Modi, O.P.; Dasgupta, R.; Yegneswaran, A.H.: Factors controlling the abrasive wear response of a zinc-based alloy silicon carbide particle composite. Compos. Part A Appl. Sci. Manuf. **28**, 301–308 (1997)

47. Murray, M.J.; Mutton, P.J.; Watson, J.D.: Abrasive wear mechanisms in steels. J. Lubr. Technol. **104**, 9–16 (1982). https://doi.org/10.1115/1.3253171

48. Hutchings, I.M.: Wear by particulates. Chem. Eng. Sci. **42**, 869–878 (1987)

49. Moore, M.A.; Douthwaite, R.M.: Plastic deformation below worn surfaces. Metall. Trans. A. **7**, 1833–1839 (1976). https://doi.org/10.1007/BF02659813

50. Wang, A.; Rack, H.J.: Abrasive wear of silicon carbide particulate and whisker-reinforced 7091 aluminium matrix composites. Wear **146**, 337–348 (1991)